Chemical Rescue of Proton Transfer in Catalysis by Carbonic Anhydrases in the β- and γ-Class†

Chingkuang Tu,‡ Roger S. Rowlett,§ Brian C. Tripp,||,⊥ James G. Ferry,|| and David N. Silverman*,‡

Departments of Pharmacology and Biochemistry, University of Florida College of Medicine, Gainesville, Florida 32610-0267, Department of Chemistry, Colgate University, Hamilton, New York 13346, and Department of Biochemistry and Molecular Biology, The Pennsylvania State University, University Park, Pennsylvania 16802-4500

Received September 10, 2002; Revised Manuscript Received October 22, 2002

ABSTRACT: Catalysis of the dehydration of HCO_3^- by carbonic anhydrase requires proton transfer from solution to the zinc-bound hydroxide. Carbonic anhydrases in each of the α, β, and γ classes, examples of convergent evolution, appear to have a side chain extending into the active site cavity that acts as a proton shuttle to facilitate this proton transfer, with His 64 being the most prominent example in the α class. We have investigated chemical rescue of mutants in two of these classes in which a proton shuttle has been replaced with a residue that does not transfer protons: H216N carbonic anhydrase from *Arabidopsis thaliana* (β class) and E84A carbonic anhydrase from the archeon *Methanosarcina thermophila* (γ class). A series of structurally homologous imidazole and pyridine buffers were used as proton acceptors in the activation of CO_2 hydration at steady state and as proton donors of the exchange of ^{18}O between CO_2 and water at chemical equilibrium. Free energy plots of the rate constants for this intermolecular proton transfer as a function of the difference in pK_a of donor and acceptor showed extensive curvature, indicating a small intrinsic kinetic barrier for the proton transfers. Application of Marcus rate theory allowed quantitative estimates of the intrinsic kinetic barrier which were near 0.3 kcal/mol with work functions in the range of 7−11 kcal/mol for mutants in the β and γ class, similar to results obtained for mutants of carbonic anhydrase in the α class. The low values of the intrinsic kinetic barrier for all three classes of carbonic anhydrase reflect proton transfer processes that are consistent with a model of very rapid proton transfer through a flexible matrix of hydrogen-bonded solvent structures sequestered within the active sites of the carbonic anhydrases.

The carbonic anhydrases catalyze the hydration of CO_2 to produce bicarbonate and a proton. Catalysis proceeds in two stages: one is the conversion of CO_2 into bicarbonate with the dissociation of bicarbonate resulting in the formation of zinc-bound water (eq 1), and the second is the regeneration of the zinc-bound hydroxide at the active site by proton transfer to solution (eq 2) (*1*−*3*). Here B indicates exogenous

$$CO_2 + EZnOH^- \rightleftarrows EZnHCO_3^- \overset{H_2O}{\rightleftharpoons} EZnH_2O + HCO_3^- \quad (1)$$

$$EZnH_2O \underset{BH^+}{\overset{B}{\rightleftharpoons}} EZnOH^- \quad (2)$$

proton acceptors in solution or a residue of the enzyme itself. To date, three classes of carbonic anhydrases, designated, α, β, and γ, have been well characterized (*4*), all of which appear to share the overall features of eqs 1 and 2 (*1*, *5*−*8*). These are examples of convergent evolution with no structural homology between classes, although each is a zinc-containing enzyme and in two cases, α and γ, three ligands coordinating the metal are histidines in a similar tetrahedral geometry (*9*, *10*). In the β class the zinc is coordinated to two Cys residues and one His residue, with a fourth ligand as either an Asp side chain or water molecule, depending on the species from which the enzyme is obtained (discussed in ref *11*).

Studies of the proton transfer reaction in catalysis by the α class of carbonic anhydrases, which includes the human and animal enzymes, have been extensive (*1*−*3*, *12*). Histidine 64 in the active site cavity of human carbonic anhydrase II (CA II) acts as a proton shuttle facilitating the transfer of protons between the active site and solution in a process that is rate-determining for the maximum velocity. The distance between the imidazole ring of His 64 and the zinc-bound water is near 7.5 Å, and proton transfer most likely occurs through intervening hydrogen-bonded water. In mutants in which His 64 is replaced by a residue that does not support proton transfer, catalysis is decreased as much as 10−100-fold and can be regenerated by addition of exogenous proton donors (*13*), a process called chemical rescue.

† This work was supported by a grant from the National Institutes of Health (GM25154 to D.N.S.).

* Address correspondence to this author at Box 100267 Health Center, University of Florida, Gainesville, FL 32610-0267. Phone: (352) 392-3556. Fax: (352) 392-9696. E-mail: silvermn@college.med.ufl.edu.

‡ University of Florida.

§ Colgate University.

|| The Pennsylvania State University.

⊥ Current address: Departments of Biological Sciences and Chemistry, Western Michigan University, Kalamazoo, MI 49008-5410.

10.1021/bi026831u CCC: $22.00
Published on Web 11/23/2002

Investigation of the catalytic properties of H216N carbonic anhydrase from *Arabidopsis thaliana* (ATCA)[1] (*11*) strongly suggests that His 216 functions as a proton shuttle during catalysis, transferring protons between the active site and solution. Studies of the analogous H208A mutant of *Pisum sativum* (pea) carbonic anhydrase are also consistent with a possible proton shuttle role for His 208 (*14*). His 208 [209 in the numbering of Kimber and Pai (*15*), who have solved the crystal structure] is 10 Å from the zinc-bound water and is completely solvent exposed. The crystal structure of carbonic anhydrase in the γ class from *Methanosarcina thermophila* (MTCA) reveals two glutamate residues (Glu 62, Glu 84) positioned in the active site cavity in a manner that suggests they may function as proton shuttle residues similar to His 64 in CA II (*10*). Catalysis by E84A MTCA reveals a pattern of catalytic properties strongly indicating that Glu 84 in MTCA also acts as a proton shuttle (*16*); the role of Glu 62 in catalysis is more complex (*16*). The distance between the zinc ion and the Cα of Glu 84 is about 9 Å in MTCA (*10*). As with CA II, proton transfer between proton shuttle residues and zinc-bound water in ATCA and MTCA probably proceeds through intervening hydrogen-bonded water, although the number of water molecules involved is not known. ATCA is a homooctamer and MTCA is a homotrimer; there is no indication from kinetic data of cooperative interaction between subunits (*8*, *11*).

The following features of catalysis by these mutants (H216N ATCA, E84A MTCA, H64A CAII) are taken to indicate a proton shuttle role for the replaced residue: compared with wild type, k_{cat} for the mutant decreased by more than 10-fold with little change in k_{cat}/K_M; k_{cat} for the mutant was activated to levels near that of wild type by exogenous proton donors/acceptors; a solvent hydrogen isotope effect greater than 2 was observed for k_{cat}, consistent with proton transfer (*11*, *13*, *16*). Enhancement of catalysis is achieved at millimolar concentrations of exogenous proton transfer donors and acceptors from solution, usually derivatives of imidazole and pyridine (*11*, *13*, *16*). In this saturable activation, the exogenous buffer acts as a second substrate for the catalysis (B of eq 2), exchanging protons between the active site and solution. This observation provides an opportunity to construct a free energy plot for this activation in which the rate constant for proton transfer between exogenous buffer and enzyme is related to the equilibrium constant for the proton transfer, as has been done for a carbonic anhydrase in the α class (*17*, *18*).

A series of studies have applied Marcus rate theory to interpret free energy plots for intramolecular proton transfer (*19*−*21*), and for intermolecular proton transfer (*17*, *18*) in catalysis by mutants of human carbonic anhydrases in the α class. The results were similar in showing that the intrinsic barrier for proton transfer is small, 0.5−2.2 kcal/mol, which can be compared with the intrinsic barrier near 2 kcal/mol for nonenzymic, bimolecular proton transfer between nitrogen and oxygen acids and bases (*22*). Moreover, catalysis by carbonic anhydrases in the α class is dominated by a large work function of 4−11 kcal/mol; this is the component of the observed free energy of activation for proton transfer that does not depend on ΔpK_a (or depends very weakly on ΔpK_a) (*12*). The similarity in Marcus parameters for these several cases of catalysis by carbonic anhydrases from the α class led us to seek another system to determine how the Marcus parameters for proton transfer would differ. The current study applies this approach to a β-class carbonic anhydrase from *A. thaliana* (H216N ATCA) and to a γ-class carbonic anhydrase from *M. thermophila* (E84A MTCA), both of which have proton transfer residues replaced with residues that do not support proton transfer. The rate constants for proton transfer were determined from the initial maximal velocity of catalyzed hydration of CO_2 measured by stopped-flow and from the catalyzed exchange of ^{18}O between CO_2 and water measured at chemical equilibrium by mass spectrometry. The Marcus parameters appear qualitatively similar to those found in the measurements of the α carbonic anhydrases, but the intrinsic kinetic barriers to intermolecular proton transfer are consistently lower than for intramolecular proton transfer. These features are interpreted in terms of the properties of the active site that promote proton transfer.

METHODS

Expression and Purification of Enzymes. The construction of the site-specific mutants, their expression in *Escherichia coli*, their purification, and the determination of enzyme concentrations are thoroughly described for H216N ATCA by Rowlett et al. (*11*) and for E84A MTCA by Tripp and Ferry (*16*).

Oxygen-18 Exchange. We used membrane-inlet mass spectrometry to measure the exchange of ^{18}O between CO_2 and water at chemical equilibrium catalyzed by H216N carbonic anhydrase from *A. thaliana* (*23*) (eqs 3 and 4). An

$$HCOO^{18}O^- + EZnH_2O \xrightleftharpoons{-H_2O} EZnHCOO^{18}O^- \rightleftarrows COO + EZnO^{18}H^- \quad (3)$$

$$EZnO^{18}H^- + BH^+ \rightleftarrows EZnH_2{}^{18}O + B \xrightarrow{+H_2O} EZnH_2O + H_2{}^{18}O + B \quad (4)$$

Extrel EXM-200 mass spectrometer with a membrane-inlet probe was used to measure the isotopic content of CO_2. Solutions contained a 25 mM total concentration of all species of CO_2.

This method gives two rates for the exchange of ^{18}O catalyzed by carbonic anhydrase based on a solution of the simultaneous kinetic equations for the ^{18}O exchange between CO_2/HCO_3^-, both singly and multiply labeled, and water (*23*). The first is R_1, the rate of exchange of CO_2 and HCO_3^- at chemical equilibrium, as shown in eq 5. Here $k_{cat}{}^{ex}$ is a

$$R_1/[E] = k_{cat}{}^{ex}[S]/(K_{eff}{}^{S} + [S]) \quad (5)$$

rate constant for maximal interconversion of substrate and product, $K_{eff}{}^{S}$ is an apparent binding constant for substrate to enzyme, and [S] is the concentration of substrate, either

[1] Abbreviations: CA, carbonic anhydrase; ATCA, carbonic anhydrase from *Arabidopsis thaliana*; H216N ATCA, the mutant of carbonic anhydrase from *A. thaliana* in which His 216 has been replaced by Asn; MTCA, carbonic anhydrase from *Methanosarcina thermophila*; HCA II, human carbonic anhydrase isozyme II; $R_1/[E]$, the rate constant for the interconversion of CO_2 and bicarbonate at chemical equilibrium as in eq 3; $R_{H_2O}/[E]$, the rate constant for the release from the enzyme of ^{18}O-labeled water as in eq 4.

CO_2 or bicarbonate. The ratio k_{cat}^{ex}/K_{eff}^{S} is, in theory and in practice, equal to k_{cat}/K_m obtained by steady-state methods (*24*).

The rate of release from the enzyme of water bearing substrate oxygen R_{H_2O} (as in eq 4) is a second rate determined by the ^{18}O exchange method. R_{H_2O} is the component of the ^{18}O exchange that is enhanced by exogenous proton donors (*23*). In such enhancements, the exogenous donor acts as a second substrate in the catalysis providing a proton (eq 4), and the resulting effect on ^{18}O exchange is described by eq 6. Here k_B^{obs} is the observed maximal rate constant for the

$$R_{H_2O}/[E] = k_B^{obs}[B]/(K_{eff}^{B} + [B]) + R_{H_2O}^{0}/[E] \quad (6)$$

release of $H_2{}^{18}O$ to bulk water caused by the addition of the buffer. K_{eff}^{B} is an apparent binding constant of the buffer to the enzyme, [E] and [B] are the concentrations of total enzyme (subunit concentration) and total buffer, and $R_{H_2O}^{0}$ is the rate of release of $H_2{}^{18}O$ into solvent water in the absence of buffer and represents the contribution to proton transfer from other sites on the enzyme or possibly solvent water itself.

A bell-shaped pH dependence of $R_{H_2O}/[E]$ is consistent with the transfer of a proton from a single predominant donor to the zinc-bound hydroxide. In these cases the pH profile is adequately fit by eq 7 in which k_B is a pH-independent

$$k_B^{obs} = k_B/\{(1 + (K_a)_{donor}/[H^+])(1 + [H^+]/(K_a)_{ZnH_2O})\} \quad (7)$$

rate constant for proton transfer and $(K_a)_{donor}$ and $(K_a)_{ZnH_2O}$ are the noninteracting ionization constants of the proton donor BH^+ of eq 4 and the zinc-bound water. An apparent second-order rate constant for the proton transfer, $(k_B/K_{eff}^{B})^{obs}$, was obtained from a fit of activation data to eq 6. An expression similar to eq 7 describes the pH profile of $(k_B/K_{eff}^{B})^{obs}$.

$$(k_B/K_{eff}^{B})^{obs} = (k_B/K_{eff}^{B})/\{(1 + (K_a)_{donor}/[H^+])(1 + [H^+]/(K_a)_{ZnH_2O})\} \quad (8)$$

Stopped-Flow Spectrophotometry. The changing pH indicator method (*25*) was used to measure initial rates of CO_2 hydration catalyzed by E84A carbonic anhydrase from *M. thermophila*. Data were taken on an Applied Photophysics SX.18MV stopped-flow spectrophotometer. Saturated solutions of CO_2 were prepared by bubbling CO_2 into water at 25 °C. Concentrations of CO_2 (0.5−17 mM) were made by diluting this saturated solution using syringes with gastight seals. We used the following buffer−indicator pairs (wavelength of observation in parentheses): 2- or 3-methylpyridine with chlorophenol red (574 nm); 3,4- or 3,5-dimethylpyridine with nitrazine yellow (589 nm); imidazole or 1-methylimidazole with 4-nitrophenol (400 nm); 4-methylimidazole with phenol red (558 nm); 2-methylimidazole with *m*-cresol purple (578 nm). Concentrations of indicators were less than 5×10^{-5} M. The total ionic strength of the solution was maintained at a minimum of 0.2 M by addition of the appropriate amount of Na_2SO_4. Initial rates are the mean of four to eight reaction traces of the first 5−10% of the reaction. The uncatalyzed rates were subtracted, and the steady-state constants k_{cat}/K_m and k_{cat} were determined by a nonlinear least-squares method (Enzfitter, Biosoft). Enhancement by exogenous proton acceptors in CO_2 hydration can be described by ping-pong kinetics (*1*, 2, *26*). Again, [E] and [B] are the concentrations of total enzyme (subunit concentration) and total buffer.

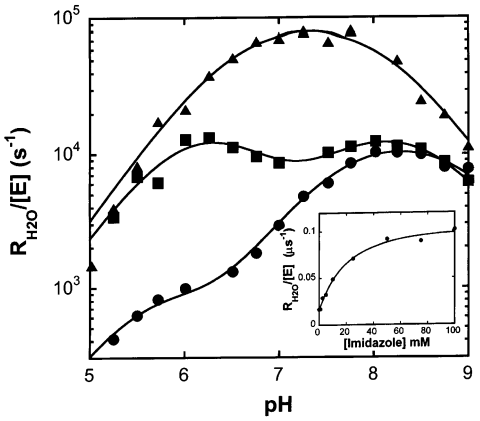

FIGURE 1: Dependence of $R_{H_2O}/[E]$ (s^{-1}) on pH for catalysis of ^{18}O exchange by (■) wild-type ATCA in the absence of exogenous proton donors, (●) H216N ATCA in the absence of exogenous proton donors, and (▲) H216N ATCA in the presence of 80 mM imidazole. Solutions contained a 25 mM total concentration of all species of CO_2 and 1 mM EDTA at 25 °C; the total ionic strength of the solution was maintained at 0.2 M by addition of Na_2SO_4. For H216N ATCA in the presence of 80 mM imidazole, the solid line is a least-squares fit of eq 7 to the data with the $pK_{a(donor)}$ of imidazole as proton donor at 6.5 ± 0.1, $pK_{a(ZnH_2O)}$ at 8.1 ± 0.2, and k_B at $(4 \pm 1) \times 10^6$ s^{-1}. Inset: Dependence of $R_{H_2O}/[E]$ (μs^{-1}) catalyzed by H216N ATCA on the concentration of imidazole. Measurements were made at pH 7.0 with other conditions as listed above.

$$\frac{v}{[E]} = \frac{k_{cat}[B]}{K_m^{B} + [B]\left(1 + \frac{K_m^{CO_2}}{[CO_2]}\right)} \quad (9)$$

At saturating CO_2

$$k_{cat}^{obs} = \frac{k_{cat}[B]}{K_m^{B} + [B]} \quad (10)$$

RESULTS

Chemical Rescue of Catalysis by H216N Carbonic Anhydrase from A. thaliana (H216N ATCA). Rowlett et al. (*11*) measured the saturable enhancement of ^{18}O exchange catalyzed by wild-type ATCA and H216N ATCA caused by the addition of the exogenous proton donor imidazole. This enhancement is manifested in $R_{H_2O}/[E]$, the rate of release of ^{18}O-labeled water from the enzyme (eq 4), and is shown in Figure 1 (inset) (see also Figure 5 of ref *11*). The pH profile for $R_{H_2O}/[E]$ catalyzed by H216N ATCA measured in the absence and presence of a saturating level of 80 mM imidazole (Figure 1) shows the enhancement caused by this exogenous proton donor over a range of pH values. The solid line shown in Figure 1 for H216N ATCA in the presence of 80 mM imidazole represents a least-squares fit of eq 7 to the data with parameters given in the legend to Figure 1. The assignment of the $pK_{a(ZnH_2O)}$ at 8.1 ± 0.2 to the ionization of the zinc-bound water is based on the pK_a determined from the pH dependence of k_{cat}/K_m for hydration of CO_2 catalyzed

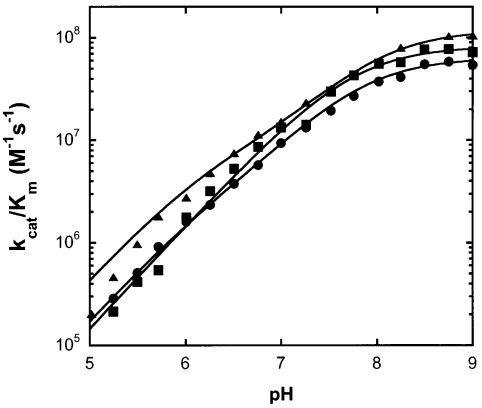

FIGURE 2: Dependence on pH of k_{cat}/K_m (M^{-1} s^{-1}) for hydration of CO_2 catalyzed by (■) wild-type ATCA in the absence of exogenous proton donors, (●) H216N ATCA in the absence of exogenous proton donors, and (▲) H216N ATCA in the presence of 80 mM imidazole. Conditions are as described in Figure 1. The values of k_{cat}/K_m were determined by ^{18}O exchange using eq 5 and setting $k_{cat}^{ex}/K_{eff}^{CO_2} = k_{cat}/K_m$. For H216N ATCA in the absence of buffer, the solid line is a fit assuming a single ionizable group with $pK_{a(ZnH_2O)} = 7.9 \pm 0.1$ and a maximal $k_{cat}/K_M = (6.2 \pm 0.3) \times 10^7$ M^{-1} s^{-1}.

by wild-type and H216N ATCA in Figure 2; this is very near the value of $pK_a = 7.8$ determined by Rowlett et al. (*11*). The apparent $pK_{a(donor)}$ at 6.5 for imidazole as a proton donor in the catalysis is also obtained from Figure 1. This is similar to the $pK_a = 7$ for unbound imidazole in solution. The rate constant for proton transfer from imidazolium to the zinc-bound hydroxide, obtained from the fit of eq 7 to the data in Figure 1, is near 4×10^6 s^{-1}.

There was no significant enhancement of k_{cat}/K_m for hydration of CO_2 by imidazole (Figure 2); in fact, there is a very slight inhibition observed for various proton donors (<5% at 100 mM imidazole; data not shown) that may be due to weak binding to the zinc, perhaps similar to that observed for the binding of imidazole to HCA I (*27*). This weak inhibition has been neglected in calculating the rate constants for proton transfer, k_B.

Similar experiments with H216N ATCA measuring the pH profile of R_{H_2O}/[E] in the presence of concentrations of other proton donors near saturation in the enhancement of catalysis gave values of pK_a similar to their solution values: 100 mM 4-methylimidazole (solution $pK_a = 7.9$; $pK_{a(donor)} = 7.6 \pm 0.1$); 80 mM 3,5-dimethylpyridine (solution $pK_a = 6.3$; $pK_{a(donor)} = 6.3 \pm 0.5$); 50 mM purine (solution $pK_a = 8.9$; $pK_{a(donor)} = 8.5 \pm 0.3$). These data demonstrate that there is not a large shift in the pK_a of the exogenous donor bound at a productive site on the enzyme. For the additional exogenous donors we used, we did not measure the entire pH profile of R_{H_2O}/[E]. For each proton donor an estimate of the maximum value of R_{H_2O}/[E] was made by fitting eq 6 to the saturable activation curve, such as shown for imidazole in Figure 1 (inset). Then, estimating the pK_a of the bound donors with their solution values and knowing $pK_{a(ZnH_2O)}$, we applied eq 7 to obtain k_B. Values of the rate constant for proton transfer, k_B, determined by these procedures are shown in the free energy plot of Figure 3. Values of the apparent second-order rate constant, k_B/K_{eff}^B, for proton transfer from various exogenous donors to zinc-bound hydroxide were determined by a fit of eqs 6 and 8 to activation data and appear in the free energy plot of Figure 4.

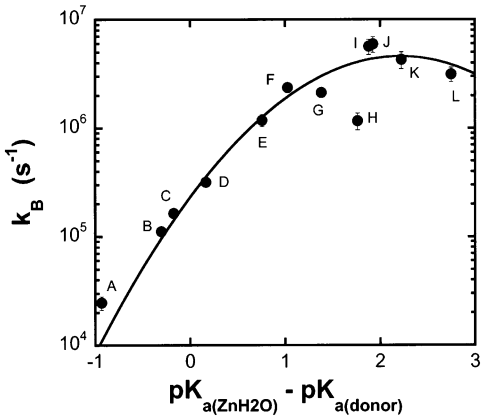

FIGURE 3: Dependence of k_B (s^{-1}), a rate constant for intermolecular proton transfer, on ($pK_{a(ZnH_2O)} - pK_{a\ (donor)}$) for catalysis of ^{18}O exchange by H216N ATCA. Experimental conditions are described in the legend of Figure 1. The value of $pK_{a(ZnH_2O)}$ is taken as 8.0. The proton donors are listed with solution values of pK_a in parentheses: A, purine (8.9); B, 1,2-dimethylimidazole (8.3); C, 2-methylimidazole (8.2); D, 4-methylimidazole (7.9); E, 1-methylimidazole (7.3); F, imidazole (7.0); G, 2,3-dimethylpyridine (6.6); H, 3,5-dimethylpyridine (6.3); I, 4-methylpyridine (6.1); J, 2-methylpyridine (6.1); K, 3-methylpyridine (5.8); L, pyridine (5.2). In each case the pH of the experiment was adjusted approximately to the pK_a of the proton donor. The solid line is a least-squares fit of the Marcus equation (eq 11) to the data, yielding the parameters given in Table 1.

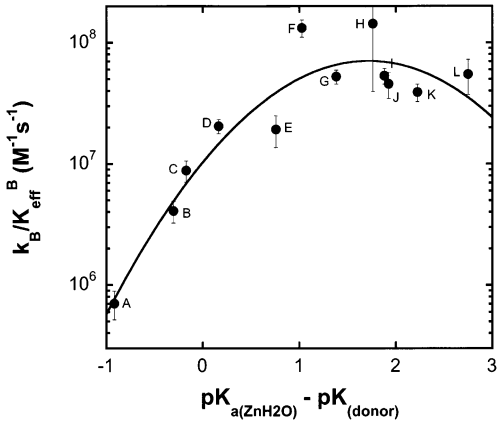

FIGURE 4: Dependence of k_B/K_{eff}^B (M^{-1} s^{-1}), an apparent second-order rate constant for proton transfer (eq 6), on ($pK_{a(ZnH_2O)} - pK_{a(donor)}$) for catalysis of ^{18}O exchange by H216N ATCA. Individual proton donors are listed in the legend of Figure 3, and experimental conditions were as listed in Figure 3. The value of $pK_{a(ZnH_2O)}$ is taken as 8.0. The solid line is a least-squares fit of the Marcus equation (eq 11) to the data, yielding parameters given in Table 1.

In reporting a similar experiment with a mutant of the α class, Y64A/F65A carbonic anhydrase V, Earnhardt et al. (*17*) found that proton transfer from pyridine derivatives methylated at the 2 position was unusually low compared with other methylated pyridines and suggested the active site pocket to be sterically hindered for these proton transfers. Such an effect with 2-substituted pyridines was not observed with H216N ATCA, presumably indicating a more open, less sterically constrained binding site for these donors.

Chemical Rescue of Catalysis by E84A Carbonic Anhydrase from M. thermophila (E84A MTCA). Bicarbonate has been shown to be a proton donor in catalysis by MTCA of the exchange of ^{18}O between CO_2 and water (*28*); hence the ^{18}O exchange method, which is carried out at chemical

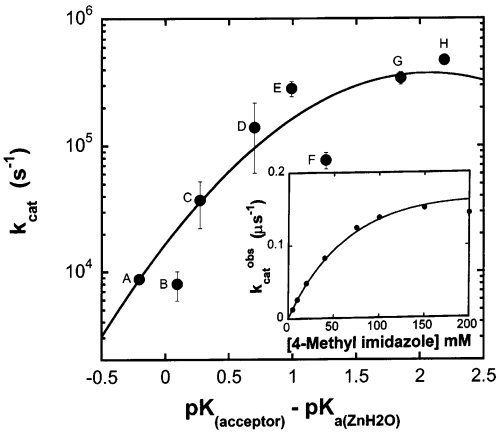

FIGURE 5: Dependence on ($pK_{a(acceptor)} - pK_{a(ZnH_2O)}$) of the maximal turnover number k_{cat} (s^{-1}) for the hydration of CO_2 catalyzed by E84A MTCA. Values of k_{cat} were obtained at 25 °C using stopped-flow spectrophotometry with solutions containing the buffers listed below and indicators as listed in Methods. The value of $pK_{a(ZnH_2O)}$ is taken as 6.0. Individual proton donors and their solution values of pK_a are as follows: A, 3-methylpyridine (5.8); B, 2-methylpyridine (6.1); C, 3,5-dimethylpyridine (6.3); D, 3,4-dimethylpyridine (6.7); E, imidazole (7.0); F, 1-methylimidazole (7.3); G, 4-methylimidazole (7.9); H, 2-methylimidazole (8.2). The total ionic strength of the solution was maintained at a minimum of 0.2 M, adjusted by adding Na_2SO_4. The solid line is a least-squares fit of the Marcus equation to all of the data, resulting in the parameters given in Table 1. Inset: Dependence of k_{cat}^{obs} (μs^{-1}) on the concentration of 4-methylimidazole at pH 7.9. Other conditions are as described above.

equilibrium with appreciable concentrations of bicarbonate, was not practicable for studies of chemical rescue. Instead, we used stopped-flow spectrophotometry to measure chemical rescue of initial velocities of CO_2 hydration at steady state catalyzed by E84A MTCA; typical data for activation by 4-methylimidazole are shown in Figure 5 (inset). Tripp and Ferry (*16*) observed the saturable activation of E84A MTCA by imidazole (Figure 3 of ref *16*).

We measured the chemical rescue of E84A MTCA by a number of proton acceptors, mostly derivatives of imidazole and pyridine. In each case, the values of k_{cat}^{obs} (eq 10) were enhanced in a saturable manner by addition of these exogenous proton acceptors. The values of k_{cat} were determined by extrapolation to saturation; there was no appreciable catalysis in the absence of these proton acceptors [as in Figure 5 (inset)]. These determinations neglected the slight inhibition of E84A MTCA by higher concentrations of these proton acceptors. These extrapolated values of k_{cat} were correlated with ΔpK_a in a free energy plot (Figure 5) with the value of $pK_a = 6.0$ for the zinc-bound water (*8*).

DISCUSSION

The approach in this work is to examine chemical rescue using carbonic anhydrases from the β and γ classes to compare with the data from the α class. The β and γ carbonic anhydrases have no structural homologies with carbonic anhydrases from the α class, being examples of convergent evolution. However, each of these classes is a zinc metalloenzyme with catalytic mechanism consistent with eqs 1 and 2. Free energy plots were constructed on the basis of the activation of chemical rescue by proton transfer mostly from derivatives of imidazole and pyridine, steps which are predominant contributors to catalysis of both ^{18}O exchange at chemical equilibrium and CO_2 hydration at steady state. The free energy plots for these measures of proton transfer appear in Figures 3 and 4 for H216N ATCA and in Figure 5 for E84A MTCA. The curved nature of these free energy plots provides a qualitative understanding of the proton transfer. According to Brønsted analysis, the slope of the plot provides information on the position of the charge in the transition state of proton transfer (*29*). The curved nature of each of these free energy plots implies a low intrinsic barrier for the proton transfer since the slope changes readily over the somewhat narrow range of ΔpK_a achieved in these experiments. In this respect these data are similar to nonenzymic proton transfers between electronegative donor and acceptor atoms such as nitrogen and oxygen acids and bases (*22*).

The value of the application of Marcus theory to these data is that it quantifies proton transfer for a series of homologous reactions that can be compared with other proton transfer systems and that it allows the separation of the kinetic and thermodynamic parts of the observed activation energy (*22*, *30*). The Marcus plot relates the overall activation energy $\Delta G^{\ddagger}$ (determined by $\Delta G^{\ddagger} = -RT \ln(hk_B/kT)$ to the measured overall free energy for the reaction given by $\Delta G^{\circ} = w^r + \Delta G_R^{\circ} - w^p$ (where $\Delta G^{\circ} = RT \ln[(K_a)_{ZnH_2O}/(K_a)_{donor}]$ for catalyzed dehydration). Here w^r is a work term in the dehydration direction, a contribution to the free energy of reaction possibly related to the energy required to align acceptor, donor, and intervening hydrogen-bonded water for facile proton transfer. The energy w^p is this work term for the reverse process in the hydration direction. The standard free energy of reaction with the active site conformation required for proton transfer is ΔG_R°. The Marcus equation (eq 11) allows us to determine an intrinsic energy barrier

$$\Delta G^{\ddagger} = w^r + (1 + \Delta G_R^{\circ}/4\Delta G^{\ddagger}_o)^2 \Delta G^{\ddagger}_o \qquad (11)$$

$\Delta G^{\ddagger}_o$, which is the value of $\Delta G^{\ddagger} - w^r$ when $\Delta G_R^{\circ} = 0$ (*30*). The solid lines of Figures 3−5 are the least-squares fit of eq 11 to the data with parameters of the Marcus equation given in Table 1. The observation that the maxima in these free energy curves appear displaced with respect to $\Delta pK_a = 0$ is a reflection of the parameters of eq 11; the maximum occurs at $\Delta G^{\circ} = w^r - w^p - 4\Delta G^{\ddagger}_o$.

The magnitude of the intrinsic barriers for intermolecular proton transfer using imidazole and pyridine donors to H216N ATCA and E84A MTCA were small with $\Delta G^{\ddagger}_o < 1$ kcal/mol (Table 1); the value of $\Delta G^{\ddagger}_o$ for E84A MTCA has greater uncertainty. These values are small like those found using the same chemical rescue agents for intermolecular proton transfer using mutants of the α-class carbonic anhydrases [Y64A/F65A CA V (*17*); H64A CA II (*18*)], also shown in Table 1. On the other hand, the case of intramolecular proton transfer from His 64, His 67, Asp 64, and Glu 64 to zinc-bound hydroxide in HCA III shows values of $\Delta G^{\ddagger}_o$ that are larger than 1 kcal/mol (Table 1) and comparable to the value near 2 kcal/mol found for nonenzymic bimolecular proton transfer between electronegative atoms (*22*).

Hence, we have found that the Marcus parameters applied to chemical rescue of carbonic anhydrase from the β and γ class are quite similar to those for several experiments with chemical rescue of carbonic anhydrases from the α class

Table 1: Comparison of Parameters of the Marcus Equation (eq 11) for Proton Transfer between the Zinc-Bound Solvent Molecule in Various Forms of Carbonic Anhydrase and Proton Transfer Groups

enzyme	proton transfer group	$\Delta G^{\ddagger}_{o}$ (kcal/mol)	$(w^{r})^{a}$ (kcal/mol)	$(w^{p})^{a}$ (kcal/mol)
H216N ATCA	exogenous[b]			
k_B (Figure 3)		0.34 ± 0.06	8.4 ± 0.4	10.0 ± 0.1
k_B/K_{eff}^{B} (Figure 4)		0.30 ± 0.07	6.7 ± 0.4	7.9 ± 0.2
E84A MTCA	exogenous[c]			
k_{cat} (Figure 5)		0.3 ± 0.1	10 ± 1	11 ± 1
H64A HCA II	exogenous[b]			
k_B[d]		0.5 ± 0.1	8.8 ± 0.1	8.5 ± 0.2
Y64A/F65A CA V	exogenous[b]			
k_B[e]		0.8 ± 0.5	10.0 ± 0.2	8.2 ± 1.0
variants of HCA III	His, Glu, Asp			
k_B (His 64)[f]		1.4 ± 0.3	10.0 ± 0.2	5.9 ± 1.1
k_B (His 67)[g]		1.3 ± 0.3	10.9 ± 0.1	5.9 ± 1.1
k_B (Glu 64 and Asp 64)[h]		2.2 ± 0.5	10.8 ± 0.1	4.0 ± 1.6

[a] In each case, this is the work function of the Marcus equation, in which w^{r} refers to the dehydration direction and w^{p} refers to the hydration. [b] These exogenous proton donors are mostly derivatives of imidazole and pyridine used in the dehydration direction, as in Figure 3. [c] These are exogenous proton acceptors used in the hydration direction. [d] An et al. (*18*). [e] Earnhardt et al. (*17*). The variant is a truncation mutant of murine CA V in which the N-terminal residue is Ser 22 in the conventional carbonic anhydrase numbering scheme. [f] Silverman et al. (*19*). [g] Ren et al. (*20*). [h] Qian et al. (*38*).

(Table 1). This is perhaps not surprising; although there are no structural homologies between these three classes, they are catalyzing the same reaction with the same mechanism and similar kinetic constants. Moreover, the Marcus parameters describing intramolecular proton transfer in the carbonic anhydrases of the α class are approximately the same when the proton donor is His 64, His 67, or Glu 64 (Table 1), most likely a result of the great variability in solvent structure that can occur between the donor and acceptor. This assumption is supported by molecular dynamics calculations on CA II, which suggest that the formation of the hydrogen-bonded water bridge between His 64 and the zinc ion can be achieved with many different structures in the water chain, some with a free energy barrier as little as 2−3 kcal/mol (*31*). The flexibility of water structures through which proton transfer proceeds may explain in part why the Marcus parameters are similar for activation of H216N ATCA, E84A MTCA, and the carbonic anhydrases of the α class in Table 1.

We now have information on a binding site for 4-methylimidazole in the active site cavity of H64A HCA II (*32*). This proton donor/acceptor forms a π-stacking interaction with the side chain of Trp5, a position that was found to be a nonproductive binding site (*18*). This result emphasized not only nonproductive binding sites but also the possibility of an array of different productive binding sites for the chemical rescue agents used in this study. The apparent second-order rate constant for proton transfer, k_B/K_{eff}^{B}, is not affected by nonproductive binding (*33*). In this respect, it is significant that the free energy plot for k_B/K_{eff}^{B} (Figure 4) also shows extensive curvature with derived Marcus parameters that are similar to those obtained from rate constant k_B.[2] Hence, nonproductive binding of the exogenous donors of Figures 3 and 4 do not appear to be predominant causes of the extensive curvature observed in these plots. One explanation for the curvature and consistently low values of $\Delta G^{\ddagger}_{o}$ found for intermolecular proton transfer reported in Table 1 is that in these experiments there are different binding sites for different rescue agents, an artifact of the experiment that results in values of $\Delta G^{\ddagger}_{o}$ that are too small.

However, there is another explanation that is also consistent with the data. That is, the values of $\Delta G^{\ddagger}_{o}$ for chemical rescue of three classes of carbonic anhydrases of unrelated active site structure represent an interpretable feature of the experiments. The low Marcus intrinsic barrier $\Delta G^{\ddagger}_{o}$ and large work functions of Table 1 indicate very efficient and rapid proton transfer occurring in a concerted manner through a hydrogen-bonded water structure present at a very low concentration. Model calculations described in terms of Marcus theory for transfer of protons between electronegative atoms through preformed water bridges show a low value of $\Delta G^{\ddagger}_{o}$, at or below 1 kcal/mol (*34*). Moreover, theoretical studies of proton transfer in a model of the active site including zinc, its histidine and water ligands, and His 64 find a single transition state indicating concerted proton transfer through a two-water bridge and dominated by quantum-mechanical tunneling (*35*). This is consistent with the small intrinsic barriers found in this work. The computed barrier for proton transfer should be close to the intrinsic barrier, which represents the magnitude of the energy barrier when the free energy of reaction is near zero, a condition which is approximated in carbonic anhydrase since the values of pK_a of imidazole and the zinc-bound water are both near 7.

Another consideration is the effect of the environment in which the proton transfer occurs. In studies of bimolecular, nonenzymic proton transfer, the magnitude of $\Delta G^{\ddagger}_{o}$ is determined by the reorganization energy of the solvent caused by the charge redistribution as the proton transfers (*36*, *37*). A change to aprotic nonaqueous solvents is found to decrease $\Delta G^{\ddagger}_{o}$ in significant part because the solvation energy is less for an aprotic solvent (*36*). In data involving carbon acids, values of intrinsic rate constants decrease by 1 or 2 orders of magnitude as solvent is changed from water to a mixed solvent containing water with increasing concentrations of dimethyl sulfoxide (*36*). It is possible that proton transfer in carbonic anhydrase is sufficiently sequestered from bulk aqueous solution that this influence of the

[2] Figures 3 and 4 show extensive curvature; however, we do not consider that we have sufficient precision or range in ΔpK_a to comment on an inverted region in these plots to which the Marcus equation is fitted.

active site cavity contributes to a low value of the intrinsic barrier. The Marcus parameters for intermolecular proton transfer in H216N ATCA and E84A MTCA in Table 1 are rather close in magnitude to those in carbonic anhydrases of the α class. This suggests that the enhanced proton transfer represented by the low values of the intrinsic barrier $\Delta G^{\ddagger}_{o}$ reflects a significant similarity in the properties of proton translocation and possibly a similarity in the active site cavities of the α, *β*, and *γ* classes of carbonic anhydrase that have evolved to promote facile proton transfer.

ACKNOWLEDGMENT

We thank Dr. A. Jerry Kresge for helpful comments and Ke Ren for excellent technical assistance.

REFERENCES

1. Lindskog, S. (1997) *Pharmacol. Ther*. *74*, 1−20.
2. Christianson, D. W., and Fierke, C. A. (1996) *Acc. Chem. Res. 29*, 331−339.
3. Silverman, D. N., and Lindskog S. (1988) *Acc. Chem. Res. 21*, 30−36.
4. Hewett-Emmett, D., and Tashian, R. E. (1996) *Mol. Phylogenet. Evol*. 5, 50−77.
5. Rowlett, R. S., Chance, M. R., Wirt, M. R., Sidelinger, D. E., Royal, J. R., Woodroffe, M., Wang, Y. A., Saha, R. P., and Lam, M. G. (1994) *Biochemistry 33*, 13967−13976.
6. Johansson, I.-M., and Forsman, C. (1993) *Eur. J. Biochem. 218*, 439−446.
7. Johansson, I.-M., and Forsman, C. (1994) *Eur. J. Biochem. 224*, 901−907.
8. Alber, B. E., Colangelo, C. M., Dong, J., Stalhandske, C. M. V., Baird, T. T., Tu, C. K., Fierke, C. A., Silverman, D. N., Scott, R. A., and Ferry, J. G. (1999) *Biochemistry 38*, 13119−13128.
9. Eriksson, A. E., Jones, T. A., and Liljas, A. (1988) *Proteins*: *Struct., Funct., Genet. 4*, 274−282.
10. Kisker, C., Schindelin, H., Alber, B. E., Ferry, J. G., and Rees, D. C. (1996) *EMBO J. 15*, 2323−2330.
11. Rowlett, R. S., Tu, C. K., McKay, M. M., Preiss, J. R., Loomis, R. J., Hicks, K. A., Marchione, R. J., Strong, J. A., Donovan, G. S., and Chamberlin, J. E. (2002) *Arch. Biochem. Biophys. 404*, 197−209.
12. Kresge, A. J., and Silverman, D. N. (1999) *Methods Enzymol. 308*, 276−297.
13. Tu, C. K., Silverman, D. N., Forsman, C., Jonsson, B. H., and Lindskog, S. (1989) *Biochemistry 28*, 7913−7918.
14. Björkbacka, H., Johansson, I.-M., and Forsman, C. (1999) *Arch. Biochem. Biophys. 361*, 17−24.
15. Kimber, M. S., and Pai, E. F. (2000) *EMBO J. 19*, 1407−1418.
16. Tripp, B. C., and Ferry, J. G. (2000) *Biochemistry 39*, 9232−9240.
17. Earnhardt, J. N., Tu, C. K., and Silverman, D. N. (1999) *Can. J. Chem. 77*, 726−732.
18. An, H., Tu, C. K., Duda, D., Montanez-Clemente, I., Math, K., Laipis, P. J., McKenna, R., and Silverman, D. N. (2002) *Biochemistry 41*, 3235−3242.
19. Silverman, D. N., Tu, C. K., Chen, X., Tanhauser, S. M., Kresge, A. J., and Laipis, P. J. (1993) *Biochemistry 32*, 10757−10762.
20. Ren, X., Tu, C. K., Laipis, P. J., and Silverman, D. N. (1995) *Biochemistry 34*, 8492−8498.
21. Tu, C. K., Qian, M. Z., Earnhardt, J. N., Laipis, P. J., and Silverman, D. N. (1998) *Biophys. J. 74*, 3182−3189.
22. Kresge, A. J. (1975) *Acc. Chem. Res. 8*, 354−360.
23. Silverman, D. N. (1982) *Methods Enzymol. 87*, 732−752.
24. Simonsson, I., Jonsson, B.-H., and Lindskog, S. (1979) *Eur. J. Biochem. 93*, 409−417.
25. Khalifah, R. G. (1971) *J. Biol. Chem. 246*, 2561−2573.
26. Rebholz, K. L., and Northrop, D. B. (1994) *Arch. Biochem. Biophys. 312*, 227−233.
27. Kannan, K. K., Petef, M., Fridborg, K., Cid-Dresdner, H., and Lovgren, S. (1977) *FEBS Lett. 73*, 115−119.
28. Tu, C. K., Tripp, C., Ferry, J. G., and Silverman, D. N. (2001) *J. Am. Chem. Soc. 123*, 5861−5866.
29. Kresge, A. J. (1975) in *Proton-Transfer Reactions* (Caldin, E. F., and Gold, V., Eds.) pp 179−199, Wiley, New York.
30. Marcus, R. A. (1968) *J. Phys. Chem. 72*, 891−899.
31. Lu, D., and Voth, G. A. (1998) *Proteins 33*, 119−134.
32. Duda, D., Tu, C. K., Qian, M., Laipis, P. J., Agbandje-McKenna, M., Silverman, D. N., and McKenna, R. (2001) *Biochemistry 40*, 1741−1748.
33. Fersht, A. (1999) in *Structure and Mechanism in Protein Science*, pp 114−116, W. H. Freeman, New York.
34. Guthrie, J. P. (1996) *J. Am. Chem. Soc. 118*, 12886−12890.
35. Smedarchina, Z., Siebrand, W., Fernandez-Ramos, A., and Cui, Q. (2002) *J. Am. Chem. Soc.* (submitted for publication).
36. Bernasconi, C. F. (1987) *Acc. Chem. Res. 20*, 301−308.
37. Staib, A., Borgis, D., and Hynes, J. T. (1995) *J. Chem. Phys. 102*, 2487−2505.
38. Qian, M., Tu, C. K., Earnhardt, J. N., Laipis, P. J., and Silverman, D. N. (1997) *Biochemistry 36*, 15758−15764.

BI026831U